Influence of surface modification on the quality factor of microresonators

O. Ergincan, G. Palasantzas,* and B. J. Kooi
Zernike Institute for Advanced Materials, University of Groningen, 9747 AG Groningen, The Netherlands
(Received 28 February 2012; revised manuscript received 1 May 2012; published 11 May 2012)

Noise measurements were performed to determine the quality factor (Q) as a function of gas pressure P for microresonators in cantilever form with systematically modified surfaces. In the free-molecular regime, which is dominated by internal energy losses, Q was substantially decreased by more than an order of magnitude with increasing surface roughness. At higher pressures, within the molecular regime, Q showed the typical inverse linear dependence on pressure $Q \sim P^{-1}$. However, in the molecular regime the Q factor also showed a strong dependence on surface morphology as indicated by surface area calculations using measured roughness data and compared to those obtained from $Q \sim P^{-1}$ plots.

DOI: 10.1103/PhysRevB.85.205420 PACS number(s): 85.85.+j, 68.55.−a, 73.50.Td, 74.62.Fj

I. INTRODUCTION

Nowadays there is relentless effort for microelectronics technology to push deep into the submicron range, which inspires the extension of microelectromechanical systems (MEMS) into the nanometer range leading to nanoelectromechanical systems (NEMS).[1–9] In this way it is possible to attain extremely high fundamental frequencies in the microwave range,[4,10] while preserving very high mechanical responsivity with mechanical quality factors $Q \sim 10^3$–10^5,[4,11] active masses of femtograms ($\sim 10^{-15}$ g),[4] heat capacities far below a yoctocalorie (10^{-18} cal),[12] etc. This combination of properties translates into high force and mass sensitivity and the potential to operate at very low power levels.[13]

Despite the enormous progress, a central theme of fundamental and applied research in MEMS/NEMS is the achievement of high Q factors. The latter is associated with damping and energy dissipation, which measures the ratio of the stored energy $E_{\rm stor}$ to the dissipated energy $E_{\rm dis}$ (within an oscillation cycle) and it is defined by the relation $Q = 2\pi(E_{\rm stor}/E_{\rm dis})$. The larger the value of Q, the higher the sensitivity of the resonance system is to external perturbations. The Q factor determines also the level of fluctuations that degrades the spectral purity of a resonance (linewidth broadening), and determines the minimum intrinsic power at which the device must operate.[4] In any case, the Q factor of a resonator is determined by the various loss mechanisms and it can be approximated by the relation $Q^{-1} = \sum_j Q_j^{-1}$. The index j includes for example attachment loss from gas molecules impinging the resonator, losses due to bulk and surface defects and impurities, thermoelastic losses (thermal currents generated by vibratory volume changes in elastic media with nonzero thermal-expansion coefficient), and losses due to phonon scattering (interaction between oscillatory sound waves and thermal phonons).[14]

In addition a variety of studies have shown that surface roughness influences the quality factor for operation in vacuum.[15–18] In Si nanowires with 45 nm beamwidths and 380 MHz resonating frequencies, the quality factor was decreased from ∼3000 to 500 by an increment of the surface area to volume ratio from ∼0.02 to 0.07.[15] Studies for SiC/Si resonators have shown that devices operational in the UHF/microwave regime had a low surface roughness (∼2.1 nm), while devices with rougher films (up to ∼7.1 nm) were operational up to the VHF range.[16] Recently it was shown theoretically that random surface roughness affects the quality factor, limit to mass sensitivity, Allan variance, and dynamic range of resonators.[17,18]

However, so far a systematic experimental study of the influence of surface roughness on the quality factor of resonators is still missing. This will be the topic of the present paper, where we explore the dependence of the Q factor on the surface morphology of commercial microcantilevers (Table I) at various gas pressures covering the whole range from the free molecular up to the continuous regime (ambient regime ∼1 atm). For our purposes the surfaces of the microcantilevers were systematically modified using ion etching in a focused ion beam (FIB), followed by surface morphology measurements using an atomic force microscope (AFM; Bruker Multimode).

II. EXPERIMENTAL PROCEDURE

The noise measurements for the determination of the Q factor were performed at room temperature using the thermal or Q-tuning method[3] and having the AFM head into a high vacuum bell-jar system with controlled pressure from ambient down to $\sim 10^{-6}$ mbar. The Q-tuning method, which was developed for the determination of cantilever spring constants (k) with accuracy down to ∼5%,[3] involves measuring the cantilever's mechanical response due to agitations of impinging molecules from the surrounding fluid (ambient air, gases at different pressures, or even liquids) and due to thermal dissipation via internal degrees of freedom.[3] The AFM hardware measures the cantilever's fluctuations as a function of time from which, by Fourier transformation, the frequency-dependent power spectral density $|A(\omega)|$ (PSD) is obtained. Fitting the PSD spectrum $|A(\omega)|$ (e.g., Fig. 1) with a Lorentzian form $|A(\omega)|^2 = A_0/[(\omega^2 - \omega_0^2)^2 + (\omega\omega_0/Q)^2]$,[3] with ω_0 the resonance frequency of the free cantilever, and after multiple data averaging of PSD spectra, the averaged Q factor (both due to intrinsic and fluidic or gas dissipation) is obtained. The noise measurements were repeated eleven times at each pressure to avoid the influence of instantaneous measurement drawbacks such as jitter effect and to confirm repeatability of the measurement. The acquired data were averaged allowing one to obtain the quality factor Q with accuracy of ∼10%. Notably, extensive analysis of cantilever heating effects in both

 ©2012 American Physical Society

TABLE I. List of investigated samples and summary of results.

No.	$l \times t$[a] (μm)	$\omega_0/2\pi$ (kHz)	k[b] (N/m)	k[a] (N/m)	S^c_{total}[b] (10^{-9} m^2)	S^d_{total}[c] (10^{-9} m^2)	Q_{int}	Q_{clamp}	Q_{TED}	Q_{surface}[d]	Q_{surf}[e]
S1	131 × 3.9	343.7	37.3	31.4	2.18	2.29	221 00	338 00	126 646	128 860	118 100
S2	132 × 4.0	342.7	38.2	32.3	2.92	2.35	223 00	323 40	123 886	174 600	119 500
S3	128 × 4.1	337.1	36.1	37.2	2.02	2.28	149 20	315 00	119 862	372 80	122 340
S4	131 × 3.9	343.8	37.3	31.4	2.20	2.34	188 32	338 00	126 631	640 20	118 100
S5	128 × 4.1	330.7	34.7	37.2	2.30	2.52	9090	315 00	122 203	142 70	122 340
S6	132 × 3.9	333.7	34.1	28.5		2.42	1495	380 20	133 784	1575	116 540

[a] w is the same for all the samples (=38 μm).
[b] S^c_{total} is calculated from the fit factor b (with a standard error ~5%–10%) shown in Fig. 2.
[c] S^d_{total} is calculated theoretically using the ρ_{rms} (S4, ~0.03; S5, ~0.35; S6, ~0.11) obtained from AFM images. For Si we have $E = 1.69 \times 10^{11}$ N/m^2, $\alpha_T = 2.6 \times 10^{-6}$ m/(m · K), $C_p = 1.64 \times 10^6$ J/(m^3 · K), $\rho = 2330$ kg/m^3, $\kappa = 148$ W/(m · K) (Ref. 22).
[d] Calculated subtracting Q^{-1}_{TED} and Q^{-1}_{clamp} from Q^{-1}_{int}.
[e] Averaged $Q_{\text{surf}} = \langle Q_{\text{surface}} \rangle$ calculated via Eq. (4) using the average value $\langle \delta E_{sl} \rangle \approx 0.9$.

air and vacuum resulted in negligible frequency shifts $\Delta\omega_0 \sim$ 10–20 Hz ($\sim 10^{-3}\%\ \omega_0$).

The insets of Fig. 1 show the AFM images of nonmodified [Fig. 1(a)] and FIB modified [Fig. 1(b)] cantilever surfaces. The write capability of FIB allows nanofabrication of grids on a specific region of the cantilever without requiring an etch mask.[19] Choosing the area of interest, without changing the cantilever width and length, the surfaces of the cantilevers are exposed to impinging Ga^+ ions in the FIB altering the surface morphology in different directions (Fig. 2; over the whole surface area of the resonator with dimensions given in Table I). Moreover, this FIB treatment was performed in such a way that the contamination and defect formation was minimized.[19] Varying the morphology with wavelike modulation parallel or perpendicular to the length of the cantilever affects the reduction of the Q factor.

III. ENERGY DISSIPATION MECHANISMS

For the noise measurements cantilevers from the same batch were used to gauge and minimize variations of the Q_{int} factor due to internal losses (Table I). The latter is given by

$$\frac{1}{Q_{\text{int}}} = \frac{1}{Q_{\text{TED}}} + \frac{1}{Q_{\text{clamp}}} + \frac{1}{Q_{\text{surface}}}, \tag{1}$$

where Q_{TED}, Q_{clamp}, and Q_{surface} denote respectively the quality factors due to thermoelastic damping, clamping losses, and surface losses.[1–9] Energy losses due to clamping (Q_{clamp}) occur because of the strain at the connection with the support base. For cantilevers with semi-infinite base or $t_b > \lambda_b$,[20] where λ_b is the wavelength of the elastic wave in the base of thickness t_b ($t_b \sim 280$ μm in our case), the Q factor is given by

$$Q_{\text{clamp}} = 0.95 \frac{l}{w} \frac{t_b^2}{t^2}, \tag{2}$$

with w and l the width and length of the cantilever, respectively. Moreover, the Q_{TED} due to thermoelastic dissipation (associated with thermal currents generated by vibratory volume changes in elastic media with nonzero thermal-expansion coefficient) is given by[21]

$$\frac{1}{Q_{\text{TED}}} = \frac{E\alpha_T^2 T}{C_p \rho} \left(\frac{6}{\zeta^2} - \frac{6}{\zeta^3} \frac{\sinh\zeta + \sin\zeta}{\cosh\zeta + \cos\zeta} \right). \tag{3}$$

E is the Young's modulus, α_T the thermal expansion coefficient, C_p the specific heat at constant pressure, T the system temperature, ρ the material density of the cantilever,

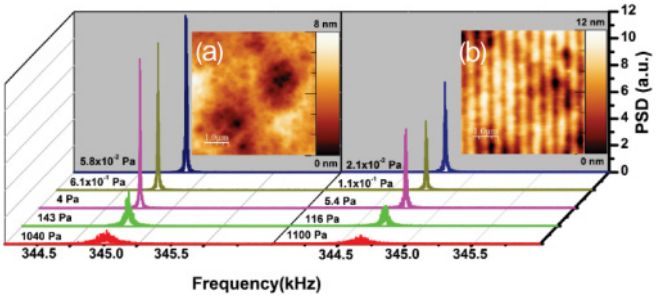

FIG. 1. (Color online) PSD spectra for various pressures from free molecular to dense regime. The graph on the left represents the nonmodified cantilever S1 and at the right-hand side shows the modified cantilever (S4) for similar pressures. Smaller amplitudes of PSDs yield lower Q factors. The insets (a) and (b) show the AFM images respectively for the smooth (S1) and the FIB roughened (S4) cantilevers.

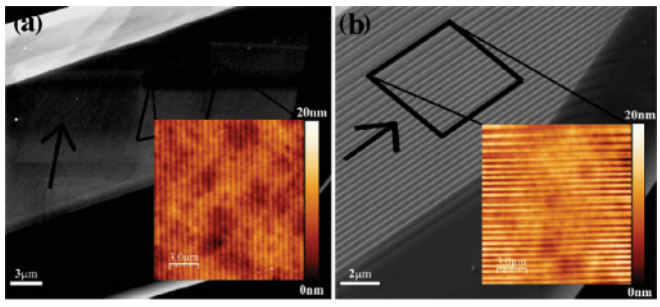

FIG. 2. (Color online) Scanning electron microscopy (SEM) and higher resolution AFM images of FIB modified surfaces (a) perpendicular to and (b) along the cantilever length as indicated by the arrows on the SEM images.

and $\zeta = t\sqrt{(\omega\rho C_p)/2\kappa}$ with κ the thermal conductivity of the cantilever.[21] Finally, we consider the surface losses to originate from a thin surface layer of complex modulus E_s due to the disruption of the atomic lattice at the surface and due to a thin layer of surface contamination.[5,21] Although this layer does not influence drastically the stored energy in the cantilever, it can enhance energy dissipation, Q_{surface}, which can be described by[5]

$$\frac{1}{Q_{\text{surface}}} = \frac{2\delta(3w+t)}{wt}\frac{E_{sl}}{E}, \tag{4}$$

with δ the thickness of the surface layer and $E_{sl} = \text{Im}[E_s]$.[5,21] The saturated or free molecular regime in Fig. 2 yields Q_{int} allowing calculation of Q_{surface} [after subtraction of Q_{TED} and Q_{clamp} obtained via Eqs. (2) and (3)]. Subsequently Eq. (4) yields the product δE_{sl} having an average value $\langle \delta E_{sl} \rangle \sim 0.9$ for the unmodified cantilevers (S1→S3; Table I). Although the cantilevers come from the same batch, δE_{sl} varies as ∼0.7–1.1 indicating variation of surface dissipation, with Q_{surface} deviating significantly from its average value Q_{surf}. The calculations are shown in Table I.

In the intrinsic region, it is the subtraction of the thermoelastic and clamping losses from the measured Q factor of the resonator which actually gives us the surface-related losses of the resonators, shown in Table I as Q_{surface}. Moreover, once the internal loss is known the essential parameter in the molecular regime is the surface area variation and not the surface contamination or surface defects (which are of secondary importance). Indeed, the first nonmodified resonator shows excellent agreement between the calculated and measured Q factors, showing that this procedure is appropriate for comparison with the modified resonators, i.e., to properly distinguish the effect of the surface modification.

Furthermore when operating in a fluid (gas or liquid), mechanical resonators generate a rapidly oscillating flow in the surrounding environment.[23] A transition from Newtonian ($\omega\tau \ll 1$) to non-Newtonian ($\omega\tau \gg 1$) flow occurs at $\omega\tau \approx 1$ with τ a fluid relaxation time ($\sim 1/P$).[23] The Newtonian approximation, the basis for the Navier-Stokes equations, breaks down also when the particulate nature of the fluid becomes significant to the flow. It is common to consider the validity of the Newtonian approximation by comparing the mean-free path λ in the medium to an ill-defined characteristic length (the width of the cantilever w) or using the Knudsen number $\text{Kn} = \lambda/w \gg 1$ (Fig. 3). For fluidic dissipation Q_{gas} is given by[23]

$$Q_{\text{gas}} = \frac{M_{\text{eff}}\omega v}{P S_{\text{total}}}\frac{1}{f(\omega\tau)} \tag{5}$$

with $f(\omega\tau) = (1+\omega^2\tau^2)^{-3/4}[(1+\omega\tau)\cos(\tan^{-1}\omega\tau/2) - (1-\omega\tau)\sin(\tan^{-1}\omega\tau/2)]$. S_{total} is the surface area of the cantilever, $v = \sqrt{k_B T/m}$ is the thermal velocity of impinging molecules with mass m, and M_{eff} is effective mass of the cantilever that vibrates.

IV. RESULTS AND DISCUSSION

In order to show that the surface area increase governs the development of the Q factor in the molecular regime we used exactly the same FIB treatment (accelerating voltage, probe current, milling time) to produce the different types of patterns. Therefore, we are able to compare the results without the need to exactly know the individual effects of surface contamination and surface defects. Figure 3 shows that in the molecular regime Q_{gas} scales with pressure P as $Q_{\text{gas}} \sim 1/P$,[24] while in the continuous regime the scaling changes to $Q_{\text{gas}} \sim 1/\sqrt{P}$.[25] The transition regime is also shown qualitatively in Fig. 4. In more detail, the total factor Q_{total} is given by $1/Q_{\text{total}} = (1/Q_{\text{int}}) + (1/Q_{\text{gas}})$, where in the molecular regime it is fitted via the relation

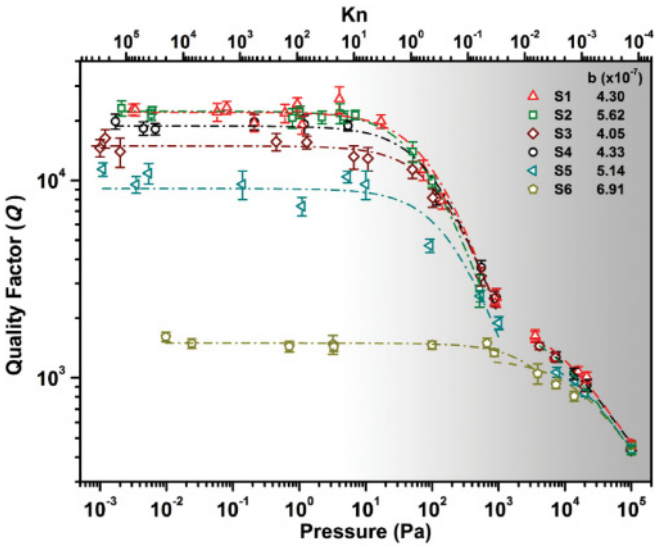

FIG. 3. (Color online) Quality factor (Q) vs P and Kn. The samples S1→S3 are nonmodified cantilevers. Samples S4 (it is the S1 modified) and S5 (it is the S3 modified) are modified cantilevers on the top surfaces but in different etching directions: (a) S4: perpendicular to the cantilever length, and (b) S5: along the cantilever length (see Fig. 2). The cantilever S6 has been modified on both the top and bottom surfaces using the same etching direction as in sample S5 (b). The fits by the solid lines illustrate the $\sim 1/P$ scaling in the molecular regime, and the $\sim 1/\sqrt{P}$ scaling in the dense or continuum regime.

$$\frac{1}{Q_{\text{total}}} = \frac{1}{Q_{\text{int}}} + b\,P \tag{6}$$

with $b = M_{\text{eff}}\omega\, v/S_{\text{total}}$. The latter yields the total effective surface area S_{total} of the cantilever. For consistency an analytical estimation of S_{total} was performed. For this we used the rough area calculation[18,25,26]

$$S_{\text{rough}}/S_{\text{smooth}} \int_0^{+\infty} du\sqrt{1+\rho_{\text{rms}}^2}\, u e^{-u} \tag{7}$$

with ρ_{rms} the average local surface slope.[27] In all cases ρ_{rms} was estimated from AFM profile analysis of cantilever surfaces. Therefore we can define the effective total surface area of the cantilever as $S_{\text{total}} = \sum_{\text{rough}}^{S} + \sum_{\text{smooth}}^{S}$. Moreover, since the cantilever's cross section is trapezoidal the area of side walls is also taken into account for the calculation of S_{total}.

A crucial parameter for the calculation of the effective area S_{total}^{c} (Table I) via the fitting factor b is M_{eff}. In

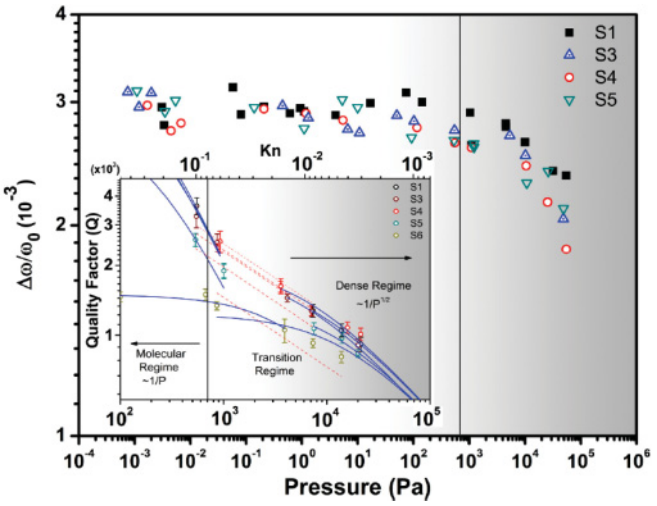

FIG. 4. (Color online) Relative frequency change $\Delta\omega_0/\omega_0$ vs P. The linear part changes at $\omega\tau \approx 1$ as is shown by the vertical solid line. The inset shows magnified the molecular to continuum transition regime. The solid (blue) lines are fits that show the change in scaling for different regimes. Dots (red) denote the scaling in the transition regime. The dotted (red) lines at the transition regime ($Q \sim P^{-1/3}$) are only meant as a guide to the eye. The samples are denoted as in Fig. 3.

order to cross-check the result, values for M_{eff} have been obtained both via theoretically and experimentally determined cantilever spring constants. Indeed, the theoretical spring constant for rectangular cantilevers with trapezoidal cross section is given by $k^a_{\text{eff}} = 3EI/l^3$ (Table I) with I the second moment of inertia.[28] Alternatively, from Q tuning one obtains the experimental cantilever spring constant k^b_{eff} (Table I).[3] Hence from the first resonance frequency of the cantilever (obtained from the maximum of the PSDs as in Fig. 1) $\omega_0 = (k^{a,b}_{\text{eff}}/M_{\text{eff}})^{1/2}$, one obtains an $M_{\text{eff}} \approx 23.5\%\, M_T$ with M_T the total mass of the cantilever.

Alternatively, the total effective surface area, denoted as S^d_{total}, is also calculated using the average local slope ρ_{rms} from AFM topography images (e.g., Figs. 1 and 2) and the expression $S^d_{\text{total}} \approx \sum S_{\text{smooth}} + \sum S_{\text{smooth}} \int_0^{+\infty} du\sqrt{1+\rho^2_{\text{rms}}u}e^{-u}$ (Table I).[26] Both results for $S^{c,d}_{\text{total}}$ agree rather well, $S^c_{\text{total}} \approx S^d_{\text{total}}$, except for sample S6 for which both top and bottom surfaces were modified. In this case only S^d_{total} can be calculated; the estimation of S^c_{total} is not feasible, because in this specific case the molecular regime, $Q_{\text{gas}} \sim 1/P$, is absent. The reason for this absence is the large energy dissipation due to intrinsic losses making the cantilever sensitive only to drastic energy losses in the continuum regime. In any case, it can be concluded that the reduction in Q within the molecular regime is associated with an increase in surface area (Table I).

The decrease in Q_{int} after altering the surface of cantilevers shows a clear change in the dominating energy dissipation mechanism in the free molecular regime which can be due to defect dissipation associated with an effective surface layer[5,21] and morphology changes. This is also depicted by the change of the PSD noise amplitude in Fig. 1 which is decreased and as we move from the molecular, to transition, and to the continuum regime where it is saturated. In addition, around the same pressure as we cross from the molecular to the continuum regime ($\omega\tau = 1$, Fig. 4), a negative frequency shift $\Delta\omega_0/\omega_0$ occurs indicating mass loading (Fig. 4). Although $\Delta\omega_0/\omega_0$ is small for relatively high frequency cantilevers the actual frequency change $\Delta\omega_0 \sim 1$ kHz is significant. Using the relation $\Delta m \approx 2(m/\omega)\Delta\omega$ one obtains a mass change $\Delta m \sim 200$ pg, which is large enough to be taken into account for the calculation of the Q factor in the continuum regime ($\omega\tau \geqslant 1$ with $\tau = 1850/P$[23].)

Finally, an important result of the present analysis is that the reduction of Q_{int} due to FIB modification is clearly affected by the type of surface morphology that is created (Fig. 2). Indeed, since both resonators in Fig. 3 have been modified in FIB using the same ion probe current and exposure time (600 pA for 5 min, respectively), one would expect a similar amount of surface contamination and ion implantation. However, when the increased surface roughness corresponds to a wavelike modulation running parallel to the length of the cantilever, the reduction of Q_{int} is clearly more pronounced than that when the modulation runs perpendicular to the cantilever length (Fig. 2). This difference is clearly a surface modification effect and it is related to the direction of wave propagation and surface scattering during resonation.[29,30] In fact the quality factor associated with dissipation due to scattering of surface acoustic waves into bulk elastic waves is strongly influenced by the presence of surface roughness.[29,30]

V. CONCLUSIONS

In conclusion, surface dissipation in the molecular regime is taken into account as a geometrical correction via the surface area calculation where our data provide a clear correlation between increasing surface area and decreasing Q factor. In the intrinsic regime the results indicate that not only surface roughness but also the direction of the surface pattern affects Q_{int}. Etching in an in-plane direction perpendicular to the wave propagation (along the width of the resonator) decreases Q_{int} less than that in the direction of wave propagation (along the length of the resonator) during resonation. Finally, extensive surface area modification of both faces of a cantilever leads to drastic reduction of Q_{int} by more than an order of magnitude and thus to high energy dissipation.

Although it is more interesting to improve Q rather than degrade it, improved understanding is one of the key factors enabling progress in this field and ultimately leading to proper Q engineering and improved Q factors. Indeed, our study shows that how you pattern resonator surfaces plays an important role in the Q factor and this has to be taken into account in sensor technologies if surface patterning is necessary.

ACKNOWLEDGMENTS

The authors would like to acknowledge financial support by STW Grant No. 10082, and useful discussions with V. B. Svetovoy.

*g.palasantzas@rug.nl

[1]A. B. Hutchinson, P. A. Truitt, K. C. Schwab, L. Sekaric, J. M. Parpia, H. G. Craighead, and J. E. Butler, Appl. Phys. Lett. **84**, 972 (2004).
[2]A. N. Cleland and M. L. Roukes, Appl. Phys. Lett. **69**, 2653 (1996).
[3]B. Ohler, Rev. Sci. Instrum. **78**, 063701 (2007).
[4]K. L. Ekinci and M. L. Roukes, Rev. Sci. Instrum. **76**, 061101 (2005).
[5]K. Y. Yasumura, T. D. Stowe, E. M. Chow, T. Pfafman, T. W. Kenny, B. C. Stipe, and D. Rugar, J. Microelectromech. Syst. **9**, 117 (2000).
[6]S. Evoy, A. Olkhovets, L. Sekaric, J. M. Parpia, H. G. Craighead, and D. W. Carr, Appl. Phys. Lett. **77**, 2397 (2000).
[7]K. L. Ekinci, Y. T. Yang, and M. L. Roukes, J. Appl. Phys. **95**, 2682 (2004).
[8]K. L. Ekinci, X. M. H. Huang, and M. L. Roukes, Appl. Phys. Lett. **84**, 4469 (2004).
[9]V. Sazonova, Y. Yaish, H. Ustunel, D. Roundy, T. A. Arias, and P. L. McEuen, Nature (London) **431**, 284 (2004).
[10]C. W. Pao and D. J. Srolovitz, Phys. Rev. Lett. **96**, 186103 (2006).
[11]C. Friesen and C. V. Thompson, Phys. Rev. Lett. **89**, 126103 (2002).
[12]I. Harald, Surf. Sci. Rep. **29**, 195 (1997).
[13]M. L. Roukes, Sci. Am. **285**(3), 48 (2001).
[14]P. Mohanty, D. A. Harrington, K. L. Ekinci, Y. T. Yang, M. J. Murphy, and M. L. Roukes, Phys. Rev. B **66**, 085416 (2002).
[15]D. W. Carr, S. Evoy, L. Sekaric, H. G. Craighead, and J. M. Parpia, Appl. Phys. Lett. **75**, 920 (1999); L. Sekaric, J. M. Parpia, H. G. Craighead, T. Feygelson, B. H. Houston, and J. E. Butler, *ibid*. **81**, 4455 (2002).
[16]X. M. H. Huang, Ph.D. thesis, California Institute of Technology, 2004, Fig 2.9, p. 36.
[17]G. Palasantzas, Appl. Phys. Lett. **90**, 041914 (2007).
[18]G. Palasantzas, Appl. Phys. Lett. **91**, 021901 (2007); J. Appl. Phys. **102**, 076111 (2007); **101**, 076103 (2007).
[19]M. Kuball, F. H. Morrissey, M. Benyoucef, I. Harrison, D. Korakakis, and C. T. Foxon, Phys. Status Solidi A **176**, 355 (1999).
[20]D. M. Photiadis and J. A. Judge, Appl. Phys. Lett. **85**, 482 (2004).
[21]R. Lifshitz and M. L. Roukes, Phys. Rev. B **61**, 5600 (2000).
[22]J. Yang, T. Ono, and M. Esashi, J. Vac. Sci. Technol. B **19**, 551 (2001).
[23]K. L. Ekinci, D. M. Karabacak, and V. Yakhot, Phys. Rev. Lett. **101**, 264501 (2008); V. Yakhot and C. Colosqui, J. Fluid Mech. **586**, 249 (2007).
[24]D. M. Karabacak, V. Yakhot, and K. L. Ekinci, Phys. Rev. Lett. **98**, 254505 (2007).
[25]O. Svitelskiy, V. Sauer, N. Liu, K.-M. Cheng, E. Finley, M. R. Freeman, and W. K. Hiebert, Phys. Rev. Lett. **103**, 244501 (2009).
[26]B. N. J. Persson, J. Chem. Phys. **115**, 3840 (2001).
[27]G. Palasantzas, Phys. Rev. B **48**, 14472 (1993); **49**, 5785 (1994); Phys. Rev. E **56**, 1254 (1997).
[28]M. A. Poggi, A. W. McFarland, J. S. Colton, and L. A. Bottomley, Anal. Chem. **77**, 1192 (2005).
[29]G. Palasantzas, J. Appl. Phys. **104**, 053524 (2008).
[30]X. Huang and A. A. Maradudin, Phys. Rev. B **36**, 7827 (1987).